A&A 376, 580–585 (2001)
DOI: 10.1051/0004-6361:20011019

Astronomy & Astrophysics

RXTE observations of single pulses of PSR B0531+21

II. Test for radio behavior

M. Vivekanand*

National Center for Radio Astrophysics, TIFR, Pune University Campus, PO Box 3, Ganeshkhind, Pune 411007, India

Received 3 May 2001 / Accepted 6 July 2001

Abstract. This article is the second in a series that analyzes about 1.87 million periods of the Crab pulsar, observed by the PCA detector aboard the RXTE X-ray observatory. At these energies, the pulsar displays none of the three phenomena that are often seen in normal radio pulsars – "pulse nulling", "systematic sub-pulse drifting" and "mode changing". The presence or absence of these three behaviors in the Crab pulsar at radio wavelengths, something that has not yet been rigorously established, might be important for a satisfactory understanding of the above three phenomena.

Key words. stars: pulsars: PSR B0531+21 – single pulses – X-ray – radio – RXTE

1. Introduction

The coherent microwave radio emission mechanism of rotation-powered pulsars is as yet an unsolved problem. The Ruderman & Sutherland (1975) model is the most successful in explaining some of the observed radio behavior. It postulates a region close to the neutron star surface that accelerates charge to relativistic energies, which produces γ-ray photons by synchrotron or related mechanism. These γ-rays produce e^+–e^- pairs in strong magnetic fields. The pairs are accelerated to relativistic energies in the same accelerator region. This process cascades into a spark of e^+–e^- pair plasma, which eventually produces the observed coherent microwave radio radiation. However the model requires a high work function of iron ions on the surface of the neutron star, which was later calculated to be too low (Hillebrandt & Mueller 1976; Flowers et al. 1977). Cheng & Ruderman (1980, and references therein) salvaged the model by invoking e^+–e^- pair production by thermal X-ray photons, emitted by the hot neutron star surface, in the Coulomb field of relativistic iron ions that are no longer bound to the neutron star surface. Therefore thermal X-ray photons probably play a significant role in the pulsar coherent radio emission mechanism.

The above models are classified as *inner-gap* (or polar cap) models, since their accelerator is just above the polar cap surface of the neutron star. However, the higher energy radiation from these pulsars (γ-rays, X-rays, infrared and optical) is now believed to originate in the *outer gaps* (Cheng et al. 1986a, 1986b, henceforth CHR; Romani & Yadigaroglu 1995), in which the accelerator is far away from the neutron star surface. This would have been a neat division of labor between the two gaps, but for the fact that the integrated profile of Crab pulsar is aligned (i.e., arrives at the same time), and also looks similar in shape, at wavelengths ranging from radio to γ-rays, except for a small part known as the radio precursor (Smith 1986; Lundgren et al. 1995; Moffet & Hankins 1996). It is now speculated that most of the Crab pulsar emission (including the radio) arises in the outer gap, while the radio precursor arises in the inner gap (CHR). In the outer gap models, the observed X-rays are produced by synchrotron processes by the *secondary* e^+–e^- pairs, which also play a role in the *bootstrap* functioning of the outer gap (CHR). Thus at least in the Crab pulsar, there appears to be an intimate connection between the coherent radio emission and the non-thermal X-ray emission (although this may not be true for, say, the Vela pulsar).

This paper looks for, in the Crab pulsar at X-ray energies, the three phenomena that are commonly observed at radio wavelengths in several normal (i.e., non-millisecond) rotation-powered pulsars – pulse "nulling", systematic sub-pulse "drifting", and integrated profile instability or "mode changing". The motivation for this analysis is to establish the direct connection, if any, between the radio and X-ray emitting relativistic charges in rotation-powered pulsars.

Consider pulse nulling; it is as yet an unexplained phenomenon. Filippenko & Radhakrishnan (1982) argue that the absence of radio emission during nulling is due to the cessation of sparking, which leads to a cessation of bunching of charges, and consequently to loss of coherence. However, the current of relativistic charges exists,

* e-mail: vivek@ncra.tifr.res.in

flowing continuously rather than as a series of sparks. Now, it is generally believed that the radio emission of rotation-powered pulsars is due to a coherent process while the higher energy emissions (optical, X-ray, γ-ray, etc.) are due to incoherent processes (see Manchester & Taylor 1977). Therefore, in the above picture, radio nulling need not be accompanied by nulling of the high energy emission. On the other hand, Kazbegi et al. (1996) think that pulse nulling is caused by "very low-frequency drift waves" that "change the curvature radius of field lines". Since a fundamental parameter is affected here, it is likely that in this scenario all emission from the pulsar will cease during nulls. The same might be true in the nulling model of Jones (1981), which postulates a reduction in the surface electric potential on the polar cap, due to a reduction in the mean nuclear charge of surface ions. Of course what exactly happens in either models will depend crucially upon the specific assumptions made and the detailed physics incorporated; but checking for the presence (or absence) of nulling at higher energies, in pulsars that exhibit radio nulling, might be an important clue to understanding the emission mechanism of rotation-powered pulsars. It would be ideal to observe such pulsars simultaneously at radio and higher energies.

Now consider mode changing. According to Filippenko & Radhakrishnan (1982) this is merely radio nulling at "certain regions of the polar gaps". Therefore in their model mode changing might not occur at all at higher energies, which can be verified by the current and similar works.

The X-ray data were obtained by the Proportional Counter Array (PCA) aboard the RXTE X-ray observatory (ObsId numbers 10203-01-01-00 to 10203-01-03-01). They consist of 23 data files observed during August/September 1996, in the EVENT mode, combining photons from all five Proportional Counter Units, and also from both halves of all three Xenon anode layers of each PCU. Channels 50 to 249 of the PCA were combined, corresponding to the energy range 13.3 to 58.4 keV. The initial data analysis used the FTOOLS software, while the latter part used self-developed software; this is explained in detail in Vivekanand 2001.

Figure 1 shows the integrated profile of Crab pulsar for 1 868 112 periods. Samples 5 to 30 are considered to represent the *on-pulse* window, and the rest of the seven samples the *off-pulse* window, although the Crab pulsar might emit X-rays all through its period. Details of the analysis in the coming sections can be found in Vivekanand (1995), Vivekanand & Joshi (1997), Vivekanand et al. (1998), Vivekanand (2000) and Vivekanand (2001); they will be described only briefly here.

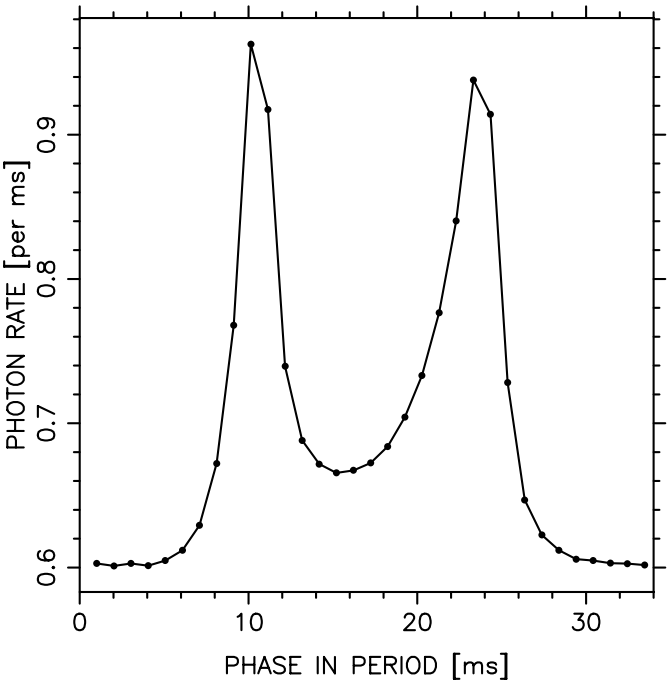

Fig. 1. Integrated profile of Crab pulsar after summing 1 868 112 periods from 23 data files of RXTE. The abscissa is time (also called phase) within the period (in ms), while the ordinate is the average number of photons obtained in one time sample (1.013967 ms; this is called "synthesized" time sample in Vivekanand 2001).

2. Pulse nulling

The coherent microwave radio radiation of some rotation-powered pulsars often ceases for durations ranging from one to several hundred periods; this is known as "pulse nulling" (Backer 1970; Ritchings 1976). During nulls the radio emission decreases by at least three orders of magnitude (Vivekanand & Joshi 1997).

Figure 2 shows the observed probability of number of photons in the off-pulse and on-pulse windows for $\approx$1 868 112 periods. The off- and on-window data fit to Poisson distributions with mean values of 3.97 and 17.57 photons, respectively; the corresponding χ^2 are 12.3 and 38.2, for 18 and 40 degrees of freedom, respectively, which implies that the fits are good.

Any nulled periods in the data will have a Poisson distribution of photons in the on-pulse window with a mean value of $3.97 \times 26 \ / \ 7 = 14.75$ photons, which is plotted as the dashed curve in the second panel of Fig. 2. The observed on-pulse window probability in the second panel (dots) will be the convolution of the nulled distribution (dashed curve) with the true non-nulled distribution, the relative weights of the two distributions depending upon the fraction of nulled periods (Ritchings 1976; Vivekanand 1995). The third panel of Fig. 2 shows the result of deconvolving the two probability distributions in the second panel. One expects the result to contain (in general) two distributions: (a) a Poisson distribution with a mean value of $17.57-14.75 = 2.82$ photons, which is plotted as the dashed curve in the third panel of Fig. 2; this represents the true, non-nulled photon distribution of the Crab pulsar in the on-pulse window, and (b) a Dirac delta function at zero photons, which represents the nulled periods, if at all (Ritchings 1976; Vivekanand 1995).

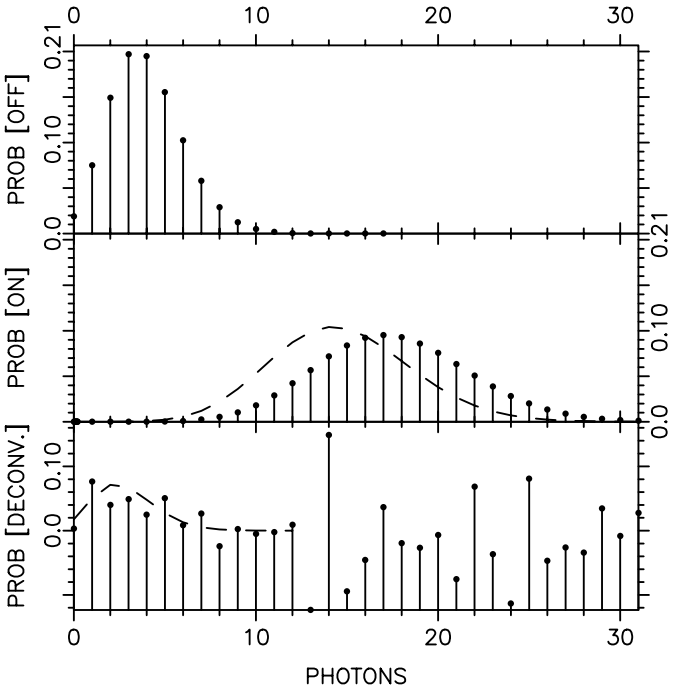

Fig. 2. Abscissa is the number of photons (observed or expected) while the ordinate is the probability of obtaining those photons. The dots in the top two panels refer to observations in the off-pulse (7 samples) and on-pulse (26 samples) windows, respectively. Dead time correction for the PCA spreads the probability over ≈6% of the abscissa around integer values, which has been corrected for. The dashed curve in the second panel is the expected (normalized) probability for nulled periods, if at all they exist, based on the off-pulse probability in the first panel. The third panel shows the result of deconvolving the observed and expected probabilities in the second panel; the dashed curve is the expected result in the absence of nulling.

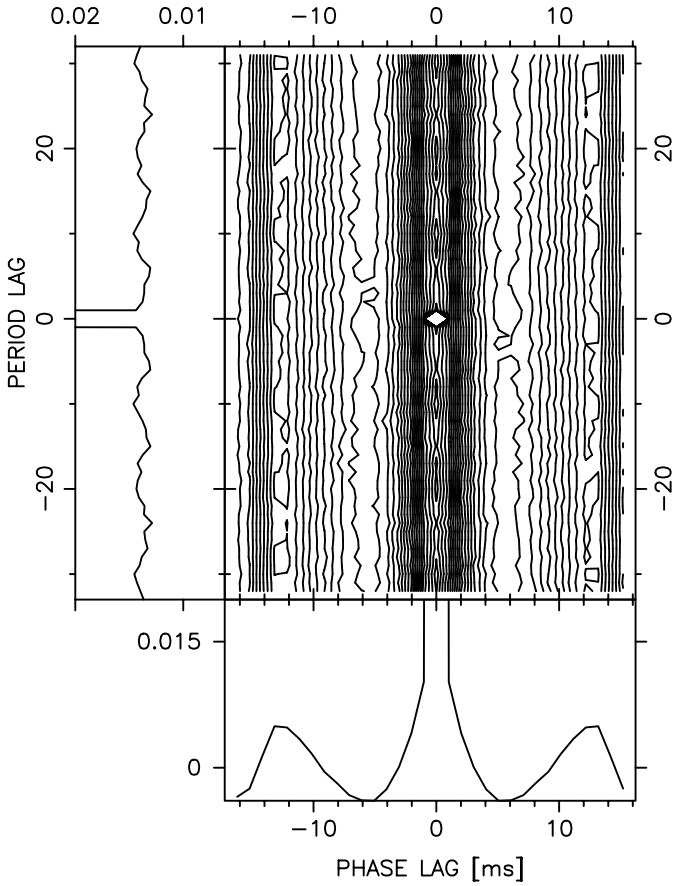

Fig. 3. Two dimensional autocorrelation of Crab pulsar X-ray flux as a function of phase and period lags, for 1 868 112 periods. Segments of two dimensional data, consisting X-ray flux at 32 time samples in 16 384 periods, were used; the details are described in Vivekanand et al. (1998). The peak autocorrelation was normalized to 1.0 in each segment before averaging. All 16 phase lags but only 32 period lags (both ± lags) have been plotted. The bottom panel is a cut at zero period lag; the secondary peaks are due to the two peaks of the integrated profile in Fig. 1. The left panel is a cut at zero phase lag. The weak quasi periodic feature is due to folding the pulsar data at a period that is not an integral multiple of the original sampling interval, which is 265 times the basic time resolution of the data (Vivekanand 2001). The synthesized sampling interval (each period has 33 such samples) differs from the former by $1.013967 - 1.010895 = 0.003072$ ms, which causes a difference of $0.003072 \times 33 / 1.013967 = 0.09998$ synthesized samples per period; this causes a periodicity of $1.0 / 0.09998 \approx 10$ periods in the data. This was confirmed by obtaining light curves with a slightly different sampling interval (1.0 ms), and folding the data as described in Vivekanand et al. (1998) (note that this method is only suitable for radio data, since it does not preserve the Poisson nature of photon statistics). The quasi periodic spectral feature almost disappeared.

Now it is well known that the deconvolution process is very sensitive to errors in the data. Clearly the deconvolution has not worked properly in Fig. 2, in spite of reducing the number of bins in the distribution, attempting a Wiener filter, etc. More data is needed for a robust result. However, the deconvolved distribution is not inconsistent with the dashed curve up to 12.0 photons along the abscissa; and there is no evidence for an excess probability (over the dashed curve) at 0.0 photons. Therefore one concludes that Crab pulsar does not display the pulse nulling phenomenon at X-ray energies. However one needs more data or better techniques for a quantitative result.

For the record, the deconvolution process had not worked either for PSR J0437-4715 in Fig. 2 of Vivekanand et al. (1998); the lower panel of their Fig. 2 shows the original distribution only. This explanation was left out inadvertently in that paper. However the nulling results of Vivekanand et al. (1998) do not change, because they were verified with a much coarser binning, where the deconvolution worked. Moreover, the deconvolution is not expected to significantly modify their original distribution, since the deconvolving function (off-pulse distribution) is about six times narrower than the function deconvolved (on-pulse distribution). In Fig. 2 above, the deconvolving function is comparable in width to the function deconvolved, which might be one of the reasons why the deconvolution is not working, in spite of the factor ≈10 or more amount of data available here.

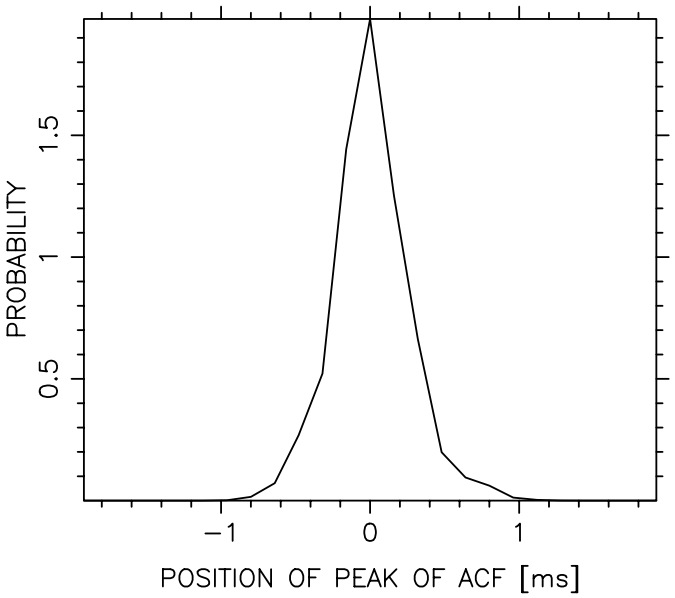

Fig. 4. Probability density of occurrence of the peak in a horizontal cut at +1 period lag in Fig. 3. Each peak is represented by a Gaussian of unit area, centered at the position of the peak, of rms width equal to the nominal error on the position. There are 25 bins along the abscissa in the range ± 2.027934 ms (2 synthesized time samples). Only those cuts with positional errors ≤0.2 ms were included.

3. Systematic sub-pulse drifting

In some rotation-powered pulsars, the radio emission is typically confined to two sub-pulses, which march across the integrated profile with each successive period. This pattern repeats periodically (see Lyne & Ashworth 1983 and Vivekanand & Joshi 1997, for two of the best examples). These are known as "drifting sub-pulses".

There are two standard methods of checking for drifting sub-pulses. One is to plot the pulsar flux as a two dimensional function of the phase within the period and the period number, and obtain the two dimensional autocorrelation. Figure 3 shows the average two-dimensional autocorrelation of Crab pulsar at X-rays; one does not notice here the characteristic sloping bands due to drifting sub-pulses.

The second method (Taylor et al. 1975) is to take cuts in Fig. 3 at period lag +1, and plot a distribution of the positions of the peaks of the autocorrelation. The sub-pulse drifting phenomenon shows up in this plot as an off centered distribution, depending upon the drift rate. Figure 4 shows that probability density for 115 such cuts (see Fig. 4 of Vivekanand et al. 1998 for the corresponding plot for PSR J0437−4715 at radio wavelengths). The distribution in Fig. 4 is quite symmetric; its mean value lies at sample 0.007 ± 0.113 ms, which is consistent with there being no systematic drifting sub-pulses as in the Crab pulsar at X-ray wavelengths.

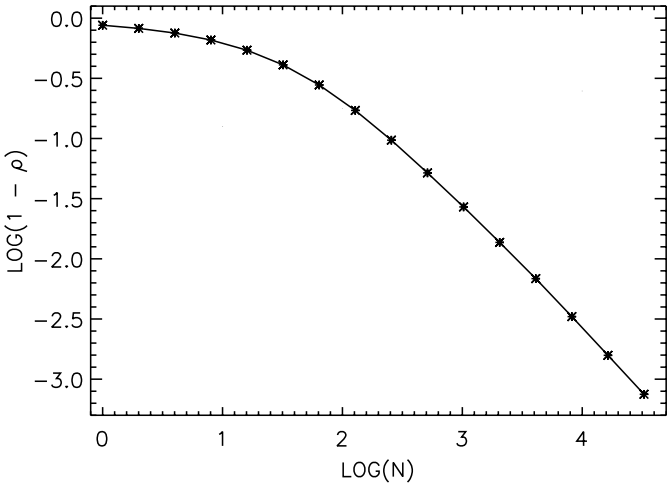

Fig. 5. Normalized correlation coefficient ρ between the master integrated profile, consisting of all 1 868 112 periods, and sub integrated profiles, consisting of N periods, both plotted in units of logarithm to the base ten. At each N there are 1 868 112 / N ρs that have been averaged. No correction has been done for background photon counts, unlike in Fig. 9 of Vivekanand et al. (1998), which has been corrected for receiver noise; however, this is not expected to introduce kinks in the above figure.

4. Stability of integrated profile

The integrated profiles of rotation-powered pulsars at radio wavelengths are generally very stable, after folding ≈100 periods. They are supposed to be as unique to pulsars as fingerprints are to humans. However, in some of them, the integrated profile changes to another stable shape, remains in that shape for ≈100 periods, before reverting back to the original integrated profile. This is known as "mode changing" (see Manchester & Taylor 1977). This should not be confused with the slower variations of integrated profiles seen in ms pulsars (Vivekanand et al. 1998; Kramer et al. 1999).

This is tested by correlating the master integrated profile, formed by folding the entire data, with sub integrated profiles consisting of N periods, for various values of N. Figure 5 shows the plot of the logarithm of $1 - \rho$, where ρ is the average correlation coefficient, as a function of logarithm of N, with N differing by powers of 2 (Helfand et al. 1975; see Fig. 9 of Vivekanand et al. 1998 for the corresponding plot for PSR J0437−4715 at radio wavelengths). The correlation ρ is very low for small N, since the X-ray emission of the Crab pulsar is dominated by photon noise.

This is in contrast to radio pulsars, where even the individual periods bear some resemblance to the integrated profile. Table 2 shows that at X-ray wavelengths, the integrated profile of the Crab pulsar requires ≈100 times more periods to stabilize, in comparison to PSR J0437−4715 at radio wavelengths. For N larger than ≈500, ρ shows no change of slope in Fig. 5, which would have been the signature of some perturbing influence on the stability of the integrated profile on those time scales (for example, mode changing). This trend continues for $N \approx 32\,000$ periods.

One can therefore conclude that the Crab pulsar does not display the mode-changing phenomenon at X-rays.

Table 1. Comparison of LOG(N) values from Fig. 5 for Crab pulsar at X-rays, and from Fig. 9 of Vivekanand et al. (1998) for PSR J0437−4715 at radio wavelengths.

LOG$(1-\rho)$	LOG(N)	
	PSR0531	PSR0437
−1.0	2.4	0.3
−2.0	3.5	1.3
−3.0	4.4	2.5

5. Discussion

The Crab pulsar does not display nulling, systematic sub-pulse drifting or mode changing at X-ray energies. Its radio behavior has not been studied so far (see Manchester & Taylor 1977). The difficulty is that Crab pulsar observations at radio wavelengths using single dishes are flooded by the continuum emission from the Crab nebula; it is difficult to obtain high signal-to-noise ratio observations of single pulses. Crab pulsar observations at radio wavelengths using interferometers will overcome this problem, but these are technically difficult observations, and no such results have been published until now (Hankins 2001).

So far, none of the above three phenomena have been given a satisfactory explanation, and they have remained essentially radio wavelength phenomena, but it is possible that similar observations at higher energies might provide the clues to resolve them.

Consider nulling first. While discussing the theoretical problems in understanding this phenomenon at radio wavelengths, Michel (1991) writes "Rather than the microphysics faltering (e.g. bunching), the global physics might falter (e.g. current flow interruption), ..." in page 68. Now, it is likely that it is the latter mechanism that might manifest itself in the high energy (e.g. X-ray) observations than the former. Therefore finding a rotation-powered pulsar that nulls either (1) at both radio and high energies, or (2) at one and not the other energy, might provide an important clue to understanding the phenomenon.

Consider next drifting sub-pulses at radio wavelengths. The Ruderman & Sutherland (1975) model invokes an electric discharge that drifts systematically in the crossed electric and magnetic fields on the polar cap. Thus, drifting is supposed to be essentially an inner-gap phenomenon; it is not clear that the electric and magnetic fields are suitable in the outer-gap for the observed drifts to occur. Now, finding a rotation-powered pulsar that shows systematic sub-pulse drifting at high energies also might be a strong constraint for the outer-gap models.

Finally, it is possible that both inner and outer gaps cannot exist simultaneously in the same rotation-powered pulsar; operation of one might extinguish the other (CHR). In that case, simultaneous radio and high energy observations of rotation-powered pulsars might be fruitful. For example, if one notices that the radio and X-ray nulls (if at all) are mutually exclusive, then one would have important information concerning the possible interplay between the two gaps, in terms of electric currents from one gap shorting out the electric fields of the other gap.

The implications of this work depend upon the radio behavior of the Crab pulsar, where none, or some or all of the above three phenomena might be found. If none of these are found in the radio, then the current results are consistent with the Crab pulsar emitting the radio and X-rays from the outer gap alone (CHR), although it would not be considered conclusive proof.

However, suppose the Crab pulsar shows the pulse nulling phenomenon in the radio; then its absence at X-rays implies that loss of coherence, or some other such physics, is responsible for nulling, while the basic relativistic charges from the Crab pulsar continue to emit the higher energies. In other words, it is the micro-physics faltering rather than the global physics. An interesting possibility is if the Crab pulsar shows nulling for a very small fraction of the time at both the radio as well as at the X-ray wavelengths, which might have been impossible to detect in this work, then the global physics would be held responsible for nulling. A much more interesting possibility would be if nulling is not simultaneous at the two wavelengths; this might necessitate the operation of both the gaps (inner and outer) in the Crab pulsar, as discussed above.

Suppose the Crab pulsar displays systematic drifting sub-pulses. Then, their absence at X-ray wavelengths might be strong evidence for the two emissions arising in the two different gaps. In other words the radio and X-ray emissions are probably highly decoupled from each other.

Acknowledgements. I thank the referee for very useful corrections and suggestions. This research has made use of (a) High Energy Astrophysics Science Archive Research Center's (HEASARC) facilities such as their public data archive, and their FTOOLS software, and (b) NASA's Astrophysics Data System (ADS) Bibliographic Services. I thank them for their excellent services.

References

Backer, D. C., 1970, Nature, 228, 42
Cheng, A. F., & Ruderman, M. A. 1980, ApJ, 235, 576
Cheng, K. S., Ho, C., & Ruderman, M. 1986a, ApJ, 300, 500 (CHR)
Cheng, K. S., Ho, C., & Ruderman, M. 1986b, ApJ, 300, 522 (CHR)
Filippenko, A. V., & Radhakrishnan, V. 1982, ApJ, 263, 828
Flowers, E. G., Ruderman, M., A., Lee, J.-F., et al. 1977, ApJ, 215, 291
Hankins, T. 2001, private communication
Helfand, D. J., Manchester, R. N., & Taylor, J. H. 1975, ApJ, 197, 661
Hillebrandt, W., & Mueller, E. 1976, ApJ, 207, 589

Kazbegi, A., Machabeli, G., Melikidze, G., & Shukre, C. 1996, A&A, 309, 515
Kramer, M., Xilouris, K. M., Camilo, F., et al. 1999a, ApJ, 520, 324
Lundgren, S. C., Cordes, J. M., Ulmer, M., et al. 1995, ApJ, 453, 433
Jones, P. B. 1981, MNRAS, 1103
Lyne, A. G., & Ashworth, M. 1983, MNRAS, 204, 519
Manchester, R. N., & Taylor, J. H. 1977, Pulsars (San Fransisco: Freeman)
Michel, F. C. 1991, Theory of Neutron Star Magnetospheres (Chicago: University of Chicago Press)
Moffet, D. A., & Hankins, T. H. 1996, ApJ, 468, 779
Ritchings, R. T. 1976, MNRAS, 176, 249
Romani, R., & Yadigaroglu, I.-A. 1995, ApJ, 438, 314
Ruderman, M. A., & Sutherland, P. G. 1975, ApJ, 196, 51
Smith, F. G. 1986, MNRAS, 219, 729
Taylor, J. H., Manchester, R. N., & Huguenin, G. R. 1975, ApJ, 195, 513
Vivekanand, M. 1995, MNRAS, 274, 785
Vivekanand, M. 2000, ApJ, 543, 979
Vivekanand, M. 2001, A&A, 373, 236
Vivekanand, M., & Joshi, B. C. 1997, ApJ, 477, 431
Vivekanand, M., Ables, J. G., & McConnell, D. 1998, ApJ, 501, 823